small NANO MICRO

Stretchable electronics

An Effective Lift-Off Method for Patterning High-Density Gold Interconnects on an Elastomeric Substrate

*Liang Guo and Stephen P. DeWeerth**

More recently, there has been a growing trend toward making electronics flexible and even stretchable,[1–7] e.g., in the applications of neural interfaces where mechanical compliance is critical.[8–12] Many challenges hinder the implementation of electronics on an elastomeric substrate with integration density and functionality comparable to that achievable on a silicon substrate. One major challenge lies in the difficulty in connecting and packaging the soft electronics with standard rigid electronics. To address this issue, we have previously developed a *via-bonding* technology to facilitate high-resolution, high-density packaging of such stretchable electronics.[13] Another major challenge to implementing high-density stretchable electronics is the fabrication of high-density interconnects on the elastomeric substrate. To increase the interconnect density, there are two necessary aspects: 1) achieving multilayer electrical interconnects within the elastomeric substrate, and 2) patterning high-density interconnects on each individual conducting layer. To address the first issue, we have implemented multilayer interconnects using an inclined-via technique.[13] For the second issue, the patterning of single 10 μm-wide gold lines on elastomeric substrates has been achieved with both wet-etching[11,14] and lift-off methods,[15] but fidelity and viability diminish as interconnect length and density increase. Although the wiring of high-density devices such as microelectrode arrays frequently requires interconnects with these characteristics, no (universally) effective solution for patterning on elastomeric substrates has been reported so far. Therefore, the focus of this paper is to present an effective method for patterning high-density thin-film gold interconnects on an elastomeric substrate, specifically polydimethylsiloxane (PDMS). We have demonstrated 10 μm-wide gold traces with a pitch as small as 20 μm for both parallel and serpentine arrangements of wires as long as 3 cm. This approach provides more than one order of magnitude improvement on the density of interconnects patterned previously on elastomeric substrates.[8,9,11,14–16]

There are many methods for patterning interconnects on PDMS, including shadow masking,[9] wet etching,[11,14] lift-off metallization,[13,15,16] laser cutting,[17] pattern transfer,[18] and printing/stamping,[19–21] among which we find the lift-off method to be the best for patterning high-density interconnects on PDMS. This is because shadow-masking, laser-cutting, pattern-transfer, and printing/stamping methods are ultimately limited in feature resolution and density, and the wet-etching method can cause problems with PDMS curing and biocompatibility.[15] In contrast, lift-off metallization has the following advantages: 1) fabrication compatibility for easy integration with other microfabrication processes to achieve devices with complex architectures, 2) capability for producing high-resolution, high-density features without limitations on pattern design (e.g., connected negative patterns as required by the shadow-masking method), and 3) no or limited exposure to contamination from etchant residuals, which is a mandatory requirement for neural implants and consumer electronics. However, material considerations limit the application of traditional lift-off processing used with rigid substrates to PDMS-based fabrication.

The fabrication difficulties stem from the unique properties of the elastomeric substrate. First, the coefficient of thermal expansion (CTE) of PDMS (310 ppm $°C^{-1}$[22]) is much higher than those of conventional photoresists used in microfabrication. As a result, when applied on PDMS substrate, these photoresists, which are optimized for application on rigid substrates (e.g., silicon and glass wafers), develop severe cracks in the film after softbake due to shrinking of the PDMS substrate. These cracks thus render the photoresist mask unusable. Second, PDMS has a loose polymeric structure that allows the absorption of chemicals and significant swelling when exposed to solvents during fabrication. The absorbed chemical residuals (e.g., etchant residuals) in the PDMS substrate can cause severe problems with regard to toxicity as well as the curing of subsequently applied negative photoresists and layers of PDMS.[15] While conventionally used as a stripper in lift-off metallization, acetone is readily absorbed by PDMS, which causes severe swelling and consequently prevents its use in lift-off processing with PDMS. This makes it hard to remove the photoresist mask. Third, PDMS surfaces have poor adhesion to conventional photoresists and thin-film metals. This limitation makes it particularly difficult to lithographically pattern high-resolution, high-density photoresist features on PDMS substrate, as the fine photoresist features would easily peel off the substrate or delaminate during development. Moreover, because of the poor adhesion of thin-film gold to PDMS substrate (even with an adhesion layer of titanium), fine gold features are likely to also delaminate from the PDMS substrate when immersed in liquids like solvents, solutions, and etchants.

In order to use the lift-off method to pattern thin-film gold interconnects on PDMS substrate, the following requirements need to be met to address the above issues associated

L. Guo, Prof. S. P. DeWeerth
The Wallace H. Coulter Department of Biomedical Engineering
Georgia Institute of Technology and Emory University
313 Ferst Drive NE, Atlanta, GA 30332–0535, USA
E-mail: steve.deweerth@gatech.edu

DOI: 10.1002/smll.201001456

with PDMS-based fabrication: 1) to avoid or dramatically reduce cracking, the photoresist used as the lift-off mask needs to have a CTE close to that of PDMS and to be strong enough to tolerate the strain developed from shrinking of the PDMS substrate during cooling down as a result of the CTE difference. 2) The patterned photoresist needs to have good adhesion to the PDMS substrate when immersed in its developer during development, especially for patterned photoresist stripes with dimensions that are very thin and long. 3) The photoresist needs to be easily removed during the lift-off process without interacting with or damaging the PDMS substrate and the desired gold features.

With these requirements in mind, we have used the negative photoresist SU-8 (CTE = 52 ppm $°C^{-1}$[23]), which is a common microfabrication material but has rarely been used for lift-off processing before. SU-8 is well-known for its capability to produce high-resolution, high-density and high-aspect-ratio features, and it adheres to PDMS strongly.[24] However, exposed and polymerized SU-8 is hard to remove; without an intermediate (sacrificial) layer, the separation of SU-8 from PDMS is difficult. Fortunately, the water soluble polymer, poly(acrylic acid) (PAA, whose dry form is used as the super-absorber in baby diapers), is reported to have good properties as a sacrificial layer for lifting off SU-8 patterns.[25] PAA dissolves rapidly in water but is insoluble in γ-butyrolactone and 1-methoxy-2-propanol-acetate (PGMEA), which are the solvents for the prepolymer resin and the developer, respectively, for bis-phenol-A-formaldehyde epoxy-based SU-8 (MicroChem Corp). Therefore, we propose a lift-off method (**Figure 1**) involving the use of SU-8 as the photoresist, PAA as an intermediate sacrificial layer, and de-ionized (DI) water as the terminal stripper for patterning high-resolution, high-density thin-film gold interconnects on PDMS substrate.

PAA adheres well to oxygen plasma treated PDMS surface, and SU-8 also adheres strongly to PAA. However, cured PAA film is brittle and vulnerable to cracking when subjected to strain. By spin-coating PAA into a thin film (~400 nm) on PDMS, we have mitigated any cracking from baking. PAA is unaffected by the photolithographic processes (spin-coating, baking, UV exposure, and development) of SU-8, and the presence of a PAA intermediate layer helps to limit the solvents (γ-butyrolactone and PGMEA) from accessing to the bulk PDMS substrate. Furthermore, PAA in the exposed areas can be easily removed by brief oxygen plasma. These properties of PAA as a sacrificial layer allow the use of SU-8 for patterning a lift-off mask with high-resolution, high-density features on PDMS, as illustrated in Figure 1a.

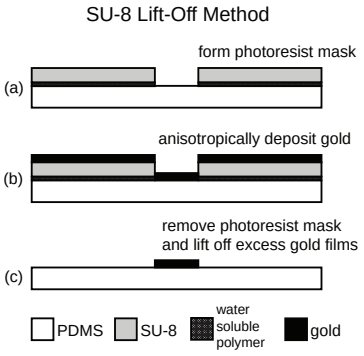

Figure 1. Lift-off method using SU-8 as the photoresist, water-soluble polymer (PAA) as an intermediate sacrificial layer, and DI water as the terminal stripper. Thin-film gold is anisotropically deposited using an electron beam evaporator.

Following thin-film coating of PAA, patterning of SU-8, plasma etching of exposed PAA, and gold evaporation (Figure 1b), the lift-off process is finally accomplished in DI water. Extensive/extended soaking of the sample in DI water to allow for complete dissolution of the PAA layer does not induce delamination of the desired fine gold features from the PDMS substrate. This observation implies that interactions of water molecules alone with the PDMS-Ti-gold interface have minimum effect on delaminating the gold thin film, while interactions from solvent molecules or ions, which potentially enter the spaces between PDMS, Ti and gold as a result of the loose structure of PDMS, have an apparent effect on delaminating the gold film.[15] Additionally, SU-8 photoresist undercuts formed from hard or soft mask contact modalities during lithography significantly speed up development, allowing the SU-8 film to be gently peeled off the sample using a pair of tweezers after soaking for 30 min in DI water, leaving the patterned gold features (Figure 1c).

Conventional SU-8 softbake and postbake protocols (e.g., softbake and postbake on a 90 °C hotplate without temperature ramping[26]) were adopted from recipes used for rigid substrates. While no cracks appeared in the SU-8 film prior to development, a variety of problems from the PDMS–PAA–SU-8 interface emerged during development, prohibiting the yield of a successful SU-8 mask. **Figure 2**a–c shows the three typical problems observed after development: microcracks in the bulk film, a major microcrack in the right-angled corner, and distortions in the SU-8 stripes, respectively. These three problems were all found to be caused by the large amount of strain embedded in the SU-8 film. During development, unexposed SU-8 was removed, and this led to imbalanced localized strain in the SU-8 film where feature edges appeared. As a result of the low mechanical modulus of the PDMS substrate, mechanical deformations of the exposed and polymerized SU-8 were allowed to partially release the embedded strain, which subsequently caused cracks and distortions in the pattern. We hypothesized that reducing the embedded strain in the SU-8 film would mitigate the above problems.

Because the glass transition temperature T_g of unexposed SU-8 is approximately 50 °C,[26] a softbake and postbake temperature of 60 °C was selected to reduce thermal strain. Further experimentations revealed that temperature ramping up and down during baking further reduced thermal stressing (see the Experimental Section for details). Figure 2e–h shows parallel traces, right-angled corners, trace terminals, and serpentine traces respectively in the improved SU-8 lift-off mask. While the remaining aggregated strain at right-angled corners was still large enough to tear the SU-8 film (Figure 2f,g), the cracks were more prominent at the lower level of the SU-8 film. Most of these cracks did not travel through the whole film (Figure 2f,g) and thus would minimally affect the patterning of gold features. The vertically non-uniform cracking was a consequence of the non-uniformly embedded strain through the SU-8 film, with the upper level having

NANO MICRO small

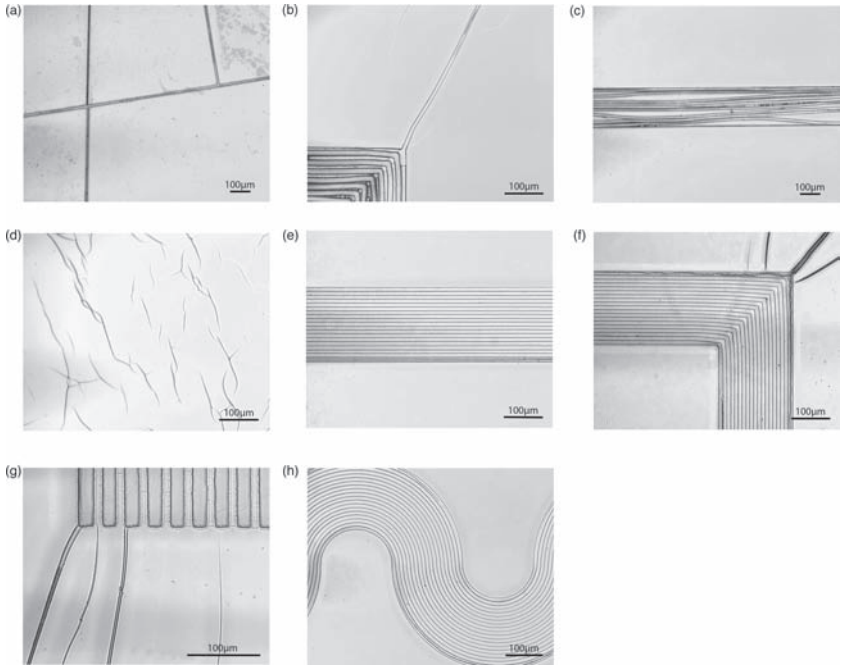

Figure 2. Patterning SU-8 lift-off mask on a PDMS substrate. Scale bars are 100 μm. a–d) Problems after development. The softbake (10 min) and postbake (5 min) were done on a 90 °C hotplate without temperature ramping up and down. a) Microcracks in the bulk SU-8 film. The residuals were a result of insufficient development and an IPA rinse. b) A major microcrack in the right-angled corner. c) Pattern distortions. d) "Nano" cracks in the bulk SU-8 film. e–h) Improved SU-8 lift-off mask. The processing recipe is detailed in the Experimental Section. A polyester film photomask was used in lithography with vacuum contact mode on the mask aligner. e,f,h) Snapshots of parallel traces, corners, and serpentine traces of 10 μm width and 20 μm pitch, respectively. The darker traces in the exposed areas of the peripheral lines were imprints of PAA cracks on PDMS. The PAA cracks were caused by intensive imbalanced strain in the adjacent SU-8 bulk film during development. PAA in the exposed areas were already removed by brief plasma etching. f) Imbalanced strain aggregated at the corner tore the film slightly apart. g) Terminals of traces of 20 μm width and 30 μm pitch. The vertically nonuniform cracks starting from the bottom surface of the SU-8 film did not go through the top surface of the film.

lower strain than the lower due to less constraint on SU-8 reflow during slow baking. Nonetheless, the selective use of rounded corners over hard corners could be designed, as the serpentine patterns showed little cracking (Figure 2h).

Another concern in the fabrication of photoresist lift-off masks is the tradeoff between high-resolution, high-density features and undercuts on photoresist feature sidewalls for an effective lift-off. Reproducibly good undercuts is one of the critical reasons for the widespread use of negative photoresists in lift-off processes. The undercut can be easily achieved during photolithography by using a non-intimate contact between the photoresist and photomask (e.g., hard contact mode on a mask aligner) combined with slight underexposure. However, with a non-intimate contact (i.e., an air gap ranging from tens of microns to more than one hundred microns will exist between the photoresist and photomask), the diffraction phenomenon of UV light starts to play an important role during lithography. Instead of a sharp boundary, the light intensity profile extends a tail from the dark-clear edge into the shadow area.[27] For negative photoresists, diffraction reduces dimensions of the unexposed features, which becomes more problematic when the unexposed features are small (as is the case for patterning the 10 μm-wide traces in Figure S2b, Supporting Information). Diffraction could also cause aliasing of the UV light intensity at the photoresist surface in the case of fine features that are densely arranged with small gaps. To faithfully pattern interconnects with very high resolution and density (e.g., 10 μm lines spaced by 10 μm gaps), intimate contact (vacuum contact mode on a mask aligner) was used during UV lithography, but a thinner 50 nm gold film (with an adhesion layer of 5 nm Ti) was deposited to ease the lift-off. For widths of traces and gaps no smaller than 20 μm, non-intimate contact (hard contact mode on a mask aligner) was used, and thicker gold film (≥100 nm, Ti:Au = 1:10) was deposited.

We used a 10 μm-thick SU-8 film as the lift-off mask, which we found to be more robust than thinner ones when peeling it off using a pair of tweezers. To take advantage of underexposure for creating better undercuts and for avoiding exposure aliasing for high-density features, for a 10 μm SU-8 film, we found that the UV exposure threshold was approximately 40 mJ cm^{-2}. Excessive underexposure was found to be one of the causes of "nano" cracks in the bulk SU-8 film during development[28] (Figure 2d). Other causes included nano air bubbles in the polyester film photomask (Figure S1a, Supporting Information), grains embedded in the SU-8 film (Figure 2d and Figure S1b), and large embedded strain in the SU-8 film. Underexposure caused insufficient polymerization of SU-8 during postbake and resulted in a weak SU-8 film. Both nano air bubbles in the polyester film photomask and grains in the SU-8 film scattered the UV light during exposure, which led to non-uniform and more attenuated exposure in the local areas. Grains also caused inconsistency in the SU-8 structure and thus induced additional irregular localized strain. Subsequently during development, the creation of imbalanced embedded strain in the patterned SU-8 film (as discussed above) generated the "nano" cracks. This problem was solved when we increased the UV exposure dose to 60 mJ cm^{-2} and used chrome-plate photomasks (Soda Lime, 0.06" thick, Nanofilm, CA and Photo Sciences, Inc., CA). We initially ordered polyester film photomasks (JD Photo-Tools, UK) and transferred the patterns onto raw chrome-plate masks (Soda Lime, 0.06" thick, Nanofilm, CA) in-house. To avoid the additional dimension errors introduced by the transfer, we used the polyester film photomask during our calibration and evaluation of the fabrication processes. We found that most of the "nano" cracks did not go through the SU-8 film, as little gold was left on the PDMS substrate at the crack patterns after lift-off. Nonetheless, for high-resolution, high-density patterns, direct-write chrome-plate photomasks are more effective.

One last point worthy of mention for successfully patterning high-resolution, high-density SU-8 features on PDMS is gentle handling of the sample during SU-8 development. To avoid introducing any potential mechanical distortions to the fine features, no agitation was applied during development, and sample rinsing was done by a gentle isopropanol (IPA) stream, followed by air drying the sample. Insufficient development and IPA rinse would leave residuals on the sample (upper right corner, Figure 2a). Without an IPA rinse, clots of dried SU-8 developer (MicroChem Corp) would contaminate the mask and cause failure regions in the lift-off. Moreover, as is sometimes recommended with SU-8 patterning, a DI water rinse should be avoided; especially considering that the rapid dissolution of water-soluble PAA causes delamination of the fine SU-8 features.

We used a polyester film photomask (vacuum contact mode) to fabricate the testing patterns in **Figure 3**, and a chrome-plate mask (hard contact mode) transferred from the polyester film mask to fabricate the patterns shown in Figure S2 (Supporting Information). The feature resolution on a polyester film is limited to 8 μm (manufacturer's specification, JD Photo-Tools, UK), and 2–3 μm on a chrome-plate mask (Photo Sciences, Inc., CA). Although we demonstrated gold traces as long as 3 cm with 10 μm width and 20 μm pitch, higher resolution and density are possible when using a high-resolution chrome-plate photomask combined with electron beam lithography and an SU-8 lift-off mask thinner than 10 μm.[29]

We fabricated numerous testing patterns with both parallel and serpentine traces. Figure 3 demonstrates the subsequently patterned gold traces from the same SU-8 lift-off mask shown in Figure 2e–h. The thickness of the gold deposition was 50 nm (primed by 5 nm Ti). Ten 3 cm parallel gold traces each with 10 μm width and 20 μm pitch were demonstrated (Figure 3a–c, see Figure S2a (Supporting Information) for the whole pattern as a reference). Ten serpentine traces spanning 2.4 cm each with 10 μm width and 20 μm pitch were demonstrated (Figure 3d,e). Such a serpentine design is shown to increase the stretchability of the interconnects.[11,18] Traces are clearly defined and free of both electrical short and open circuits (**Figure** 3a,b,d and **4**a). Nonthrough cracks at right-angled corners (Figure 2f,g) left imprints on the PDMS substrate (Figure 3a,b). Closer inspections revealed minimal gold residuals on these imprints, with some exceptions (corner of Figure 3a).

To systematically evaluate electrical properties of the patterned interconnects, two sets of experiments were conducted: 1) impedance spectroscopy on high-density parallel traces (10 μm wide with 20 μm pitch) versus isolated single traces to reveal any potential problems with the high-density parallel traces, and 2) uniaxial stretching experiments to characterize the evolution of electrical resistance under tensile strain. Figure 4a shows the normalized average impedance spectra with boundaries of one standard deviation for the ten parallel traces and ten single traces. The two spectra overlaped with each other when plotted in the same plot. This overlap verified that there existed no multiple-site (≥2) short circuits or cross-talks between the adjacent parallel traces. Further impedance measurements between any two adjacent traces each resulted in an open circuit, thus eliminating the possibility of single-site short circuits. Therefore, the high-density parallel traces patterned are electrically equivalent to isolated single traces with the same dimensions.

Since the impedance spectroscopy experiment revealed statistically constant impedance of the interconnect across the frequency spectrum (Figure 4a), in the uniaxial stretching experiments, simple resistance measurement was employed. Figure 4b shows the resistance variations under longitudinal strain for 2 cm long, 100 μm wide, flat straight traces with difference thicknesses. Flat straight traces with a thickness no smaller than 100 nm failed at longitudinal tensile strain slightly greater than 1%, while those with a thickness of 50 nm could withstand tensile strain up to 2%. These results agree with the properties of free-standing thin metal films[2] and are consistent with our previous study on gold interconnects patterned with a wet-etching method,[11] but the stretchability is considerably low compared to works on flat straight traces from other groups.[1,2] This discrepancy may be a result of different micro/nano-scale morphologies of the gold films deposited with different equipment under different conditions.[30] For example, we deposited the gold film in an e-beam evaporator at 1 Å s^{-1}, which was found to result in a denser film than higher rates and to promote gold adhesion to PDMS,[15] while 2 Å s^{-1} was used in References [1] and [2]. Many other factors, including thickness of

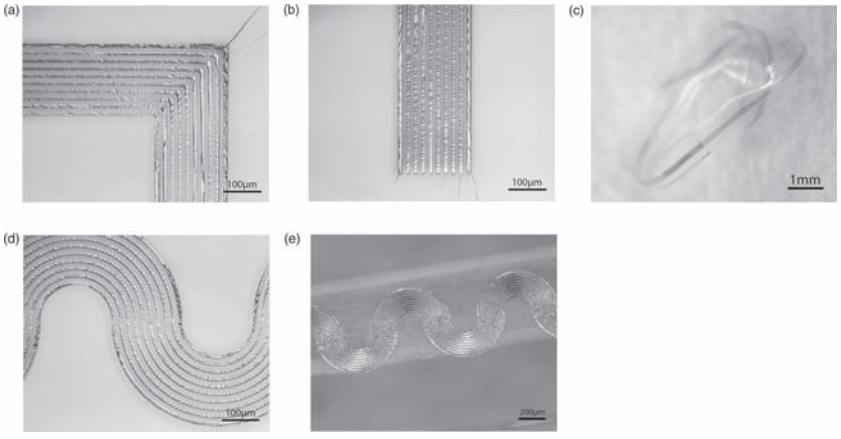

Figure 3. Lift-off results. The same sample as shown in Figure 2e–h was used to produce these results. 50 nm gold was deposited. Different testing patterns were designed on the same polyester film photomask to evaluate the fabrication resolution and density, but only the details of traces with the highest resolution and density (10 μm width and 20 μm pitch) are shown here. For a complete set of results from a sample patterned using a chrome-plate mask, please see Figure S2 in the Supporting Information. a,b,d) Low-amplitude wrinkles displayed in the gold traces. Scale bars are 100 μm. Close inspections of (a) and (b) revealed that the traces at the corner and terminals, except the major one in (a), were imprints of SU-8/PAA cracks on PDMS, not deposited gold residuals. c,e) The 3 cm and 2.4 cm stripes each containing ten 10 μm wide traces with 20 μm pitch in parallel and serpentine arrangement, respectively, were cut out with a razor blade and peeled off the glass. c) The parallel stripe was curled using a pair of tweezers to get an overview of the whole stripe. Scale bar is 1 mm. e) The serpentine stripe was slightly stretched (~2%). Scale bar is 200 μm.

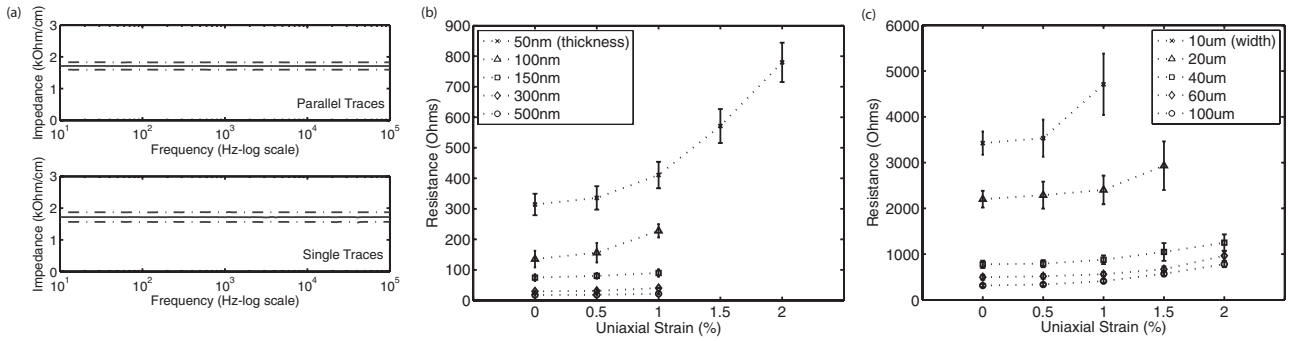

Figure 4. Electrical properties of patterned interconnects. a) Normalized average impedance spectra (solid line) of ten 50 nm-thick, 10 μm-wide parallel traces with 20 μm pitch (top plot) and ten 50 nm-thick,10 μm-wide isolated single traces (bottom plot). One standard deviations from the average were shown as the dash-dotted lines. b) Resistance variations under uniaxial (longitudinal) strain for 2 cm long, 100 μm wide, flat straight traces with difference thicknesses. c) Resistance variations under uniaxial (longitudinal) strain for 2 cm long, 50 nm thick, flat straight traces with different widths.

the PDMS substrate (70 μm was used in our experiments), may also play a role.

Figure 4c shows the resistance variations under longitudinal strain for 2 cm long, 50 nm thick, flat straight traces with different widths. Traces with width of 40 μm and above could withstand tensile strain up to 2%, while narrower traces broke at slightly lower strain (1% strain for 10 μm wide traces, and 1.5% for 20 μm traces, respectively). This was probably because the microcracks that were induced by tensile strain and responsible for electrical failure[31] were easier to develop across the full width of narrower traces.

For all samples tested, when relaxed below the critical strain for causing electrical failure, the trace re-conducted, albeit that the resistance became slightly higher than before at same strain. This recovery phenomenon is consistent with previous observations.[1,2,11,16,18,31]

In conclusion, we have developed an effective lift-off method for patterning high-resolution, high-density, thin-film gold interconnects on a PDMS substrate. We fabricated both parallel and serpentine gold traces with 10 μm width and 20 μm pitch, successfully demonstrating density increases of more than one order of magnitude from previously established work. Higher resolution and density are likely possible with the use of high-resolution chrome-plate photomasks combined with electron beam lithography. Electrical tests verified that the high-density interconnects are electrically equivalent to isolated single interconnects with the same dimensions. Uniaxial stretching experiments revealed that the patterned, flat, straight thin-film gold interconnects could withstand longitudinal tensile strain in the range of 1 ~ 2%. To further boost stretchability, structures that facilitate large mechanical deformations[32] can potentially be incorporated into the interconnect design to create, e.g., serpentine traces[11,18] (as already demonstrated), wavy traces,[1,2] or ion-implanted traces.[33] Many applications in the fields of stretchable electronics and conformable neural interfaces will benefit from the fabrication developments present here.

Experimental Section

Materials: PDMS (Sylgard 184) was purchased from a distributor of Dow Corning Corp. SU-8 2007 and SU-8 Developer were purchased from MicroChem Corp. PAA (50 kDa) was purchased from Polysciences, Inc. (Warrington, PA) as a 25% (w/v) solution in water, and diluted with DI water to 10% (w/v).[25]

Polyester film photomasks were self-designed using AutoCAD 2007 (Autodesk, Inc.) and ordered from JD Photo-Tools, UK. The patterns were also transfered onto raw chrome-plate masks (Soda Lime, 0.06" thick, Nanofilm, CA) in-house using a Karl Suss MA-6 Mask Aligner with vacuum contact mode. High-resolution chrome-plate masks (Soda Lime, 0.06" thick) were self-designed and directly ordered from Photo Sciences, Inc., CA.

SU-8 Lift-Off Method: PDMS was prepared by mixing the base and curing agent at 10:1 weight ratio. The prepolymer was left at room temperature for 40 min for the dissipation of air bubbles. The de-aired prepolymer was spin-coated onto a cleaned glass slide (precoated with 1 nm Ti/ 5 nm Au) for the desired thickness[34] (70 μm in the current experiments) and cured on a hotplate. Following brief oxygen plasma treatment of the PDMS surface, PAA 10% (w/v) solution was spin-coated at 4000 rpm for 15 s and baked on a hotplate at 60 °C for 5 min to yield a film of ~400 nm.[25] The sample was cooled down for 2 min, and SU-8 2007 was immediately spin-coated at 1500 rpm for 30 s. Then the sample was placed on a hotplate slowly ramping from room temperature to 60 °C at a rate of 5 °C h^{-1}, held for 1 h, and then cooled down to room temperature by automatically turning off the hotplate. The resulting SU-8 thickness was ~10 μm. In the photolithography process, the sample was patterned with a UV exposure dose of 60 mJ cm^{-2}, post-baked on a hotplate at 60 °C for 30 min with a ramp up rate of 5 °C h^{-1} from room temperature, cooled down to room temperature by automatically turning off the hotplate, developed in SU-8 Developer for ~150 s, gently rinsed with an IPA stream, and dried in air. It was necessary to leave the sample in air for at least 12 h to allow the solvent residues to fully evaporate. PAA in the exposed areas was then removed using brief plasma etching (O_2/SF_6 = 20/1, 150 mTorr, 200 mW, 1 min) (Figure 1a). A layer of 50 ~ 500 nm gold was deposited in an e-beam evaporator at 1 Å s^{-1} with a titanium adhesion layer of 1/10 gold thickness (Figure 1b). The lift-off was done in DI water. After soaking for a few hours, the SU-8 film was gently peeled off in DI water using a pair of tweezers, leaving the patterned gold features (Figure 1c).

Impedance Spectroscopy: To test electrical properties of 10 μm wide, 20 μm pitch parallel traces, which is the currently achievable fabrication limit, a new chrome-plate mask was ordered commercially (Photo Sciences, Inc., CA). Two classes of patterns were

designed on this mask: 1) ten 3 cm parallel traces with 10 μm width and 20 μm pitch, and 2) isolated single 3 cm traces with 10 μm width. The parallel traces each were joined by 10 μm-wide traces at the two terminals which then fanned out to contact pads. The fanning-out routes at either end had a length in the range of 0.5–1.25 cm, which were taken into account during the impedance normalization. For the single traces, one contact pad was directly attached to each end. Samples, with their glass slide attached for the ease of handling, were probed on the contact pads, while impedance spectra measured using a spectrum analyzer (SRS Dynamic Signal Analyzer, SR785).

Stretching Experiments: To test electrical properties of the patterned gold interconnects under longitudinal tensile strain, a chrome-plate mask was designed with a set of 2 cm wires of different widths (10, 20, 40, 60, and 100 μm). One 4 mm^2 square contact pad was attached to each terminal of every wire (see Figure S3c, Supporting Information). Samples were fabricated with gold film thickness of 50, 100, 150, 300, and 500 nm (the Ti adhesion layer was of 1/10 gold thickness), respectively. Figure S3 shows the stretching experiment setup. Micromanipulators (Siskiyou, Inc., OR) were used to mount and stretch PDMS-based gold interconnects, while the resistances were monitored by a multimeter (Figure S3a). A microscope was used to visually check the contact between probing wires and gold contact pads, as well as the status of the interconnect under stretching. Two copper wires (200 μm in diameter) each connected to one multimeter probe touched on the two contact pads (Figure S3b,c) to form a closed circuit. The tip of each copper wire was bent to a hook shape to avoid damaging the contact pad (Figure S3c). The contact resistances together with the resistances of probe wires were measured for each gold film thickness, by touching the two copper wires on the same contact pad, and subtracted from the interconnect resistances during data analysis. For each data point in Figure 4b,c, four individual samples each with a flat straight interconnect were tested.

Supporting Information

Supporting Information is available from the Wiley Online Library or from the author.

Acknowledgements

This research was supported by US National Institutes of Health (Grant# EB006179). The authors would like to thank Dr. M. A. McClain and B. Wester for providing valuable comments on the manuscript.

[1] S. P. Lacour, J. E. Jones, S. Wagner, T. Li, Z. Suo, *Proc. IEEE* **2005**, *93*, 1459–1467.
[2] S. Wagner, S. P. Lacour, J. Jones, P.-H. I. Hsu, J. C. Sturm, T. Li, Z. Suo, *Physica E* **2004**, *25*, 326–334.
[3] H. C. Ko, M. P. Stoykovich, J. Song, V. Malyarchuk, W. M. Choi, C.-J. Yu, J. B. Geddes III, J. Xiao, S. Wang, Y. Huang, J. A. Rogers, *Nature* **2008**, *454*, 748–753.
[4] D.-H. Kim, J.-H. Ahn, W. M. Choi, H.-S. Kim, T.-H. Kim, J. Song, Y. Y. Huang, Z. Liu, C. Lu, J. A. Rogers, *Science* **2008**, *320*, 507–511.
[5] S.-I. Park, Y. Xiong, R.-H. Kim, P. Elvikis, M. Meitl, D.-H. Kim, J. Wu, J. Yoon, C.-J. Yu, Z. Liu, Y. Huang, K.-C. Hwang, P. Ferreira, X. Li, K. Choquette, J. A. Rogers, *Science* **2009**, *325*, 977–981.
[6] T. Someya, Y. Kato, T. Sekitani, S. Iba, Y. Noguchi, Y. Murase, H. Kawaguchi, T. Sakurai, *Proc. Natl Acad. Sci. USA* **2005**, *102*, 12321–12325.
[7] T. Sekitani, Y. Noguchi, K. Hata, T. Fukushima, T. Aida, T. Someya, *Science* **2008**, *321*, 1468–1472.
[8] M. Maghribi, J. Hamilton, D. Polla, K. Rose, T. Wilson, P. Krulevitch, *2nd Ann. Int. IEEE-EMB Spec. Top. Conf. Microtechnol. Med. Biol.* **2002**, 80–83.
[9] S. P. Lacour, C. Tsay, S. Wagner, Z. Yu, B. Morrison III, *Proc. 4th IEEE Conf. Sensors* **2005**, 617–620.
[10] D. C. Rodger, A. J. Fong, W. Li, H. Ameri, A. K. Ahuja, C. Gutierrez, I. Lavrov, H. Zhong, P. R. Menon, E. Meng, J. W. Burdick, R. R. Roy, V. R. Edgerton, J. D. Weiland, M. S. Humayun, Y.-C. Tai, *Sens. Actuators B* **2008**, *132*, 449–460.
[11] K. W. Meacham, R. J. Giuly, L. Guo, S. Hochman, S. P. DeWeerth, *Biomed. Microdevices* **2008**, *10*, 259–269.
[12] D.-H. Kim, J. Viventi, J. J. Amsden, J. Xiao, L. Vigeland, Y.-S. Kim, J. A. Blanco, B. Panilaitis, E. S. Frechette, D. Contreras, D. L. Kaplan, F. G. Omenetto, Y. Huang, K.-C. Hwang, M. R. Zakin, B. Litt, J. A. Rogers, *Nat. Mater.* **2010**, *9*, 511–517.
[13] L. Guo, S. P. DeWeerth, *Adv. Mater.* **2010**, *22*, 4030–4033.
[14] T. Adrega, S. P. Lacour, *J. Micromech. Microeng.* **2010**, *20*, 055025.
[15] L. Guo, K. W. Meacham, S. Hochman, S. P. DeWeerth, *IEEE Trans. Biomed. Eng.* **2010**, *57*, 2485–2494.
[16] M. A. McClain, M. C. LaPlaca, M. G. Allen, *J. Micromech. Microeng.* **2009**, *19*, 107002.
[17] M. Schuettler, S. Stiess, B. V. King, G. J. Suaning, *J. Neural Eng.* **2005**, *2*, S121–S128.
[18] D. S. Gray, J. Tien, C. S. Chen, *Adv. Mater.* **2004**, *16*, 393–397.
[19] S. Tawfick, K. O'Brien, A. J. Hart, *Small* **2009**, *5*, 2467–2473.
[20] C.-X. Liu, J.-W. Choi, *J. Micromech. Microeng.* **2009**, *19*, 085019.
[21] K. S. Kim, Y. Zhao, H. Jang, S. Y. Lee, J. M. Kim, K. S. Kim, J.-H. Ahn, P. Kim, J.-Y. Choi, B. H. Hong, *Nature* **2009**, *457*, 706–710.
[22] M. V. Kunnavakkam, F. M. Houlihan, M. Schlax, J. A. Liddle, P. Kolodner, O. Nalamasu, J. A. Rogers, *Appl. Phys. Lett.* **2003**, *82*, 1152–1154.
[23] S. Tuomikoski, S. Franssila, *Sens. Actuators A* **2005**, *120*, 408–415.
[24] Y. Xia, G. M. Whitesides, *Angew. Chem. Int. Ed.* **1998**, *37*, 550–575.
[25] V. Linder, B. D. Gates, D. Ryan, B. A. Parviz, G. M. Whitesides, *Small* **2005**, *1*, 730–736.
[26] A. L. Bogdanov, *Proc. SPIE* **2000**, *3999*, 1215.
[27] Y. Cheng, C.-Y. Lin, D.-H. Wei, B. Loechel, G. Gruetzner, *IEEE J. Microelectromechanical Sys.* **1999**, *8*, 18–26.
[28] MicroChem, product data sheet.
[29] L. J. Millet, M. E. Stewart, R. G. Nuzzo, M. U. Gillette, *Lab Chip* **2010**, *10*, 1525–1535.
[30] O. Graudejus, P. Gorrn, S. Wagner, *Appl. Mater. Interfaces* **2010**, *2*, 1927–1933.
[31] S. P. Lacour, D. Chan, S. Wagner, T. Li, Z. Suo, *Appl. Phys. Lett.* **2006**, *88*, 204103.
[32] J. A. Rogers, T. Someya, Y. Huang, *Science* **2010**, *327*, 1603–1607.
[33] S. Rosset, M. Niklaus, P. Dubois, H. R. Shea, *Adv. Funct. Mater.* **2009**, *19*, 470–478.
[34] A. Mata, A. J. Fleischman, S. Roy, *Biomed. Microdevices* **2005**, *7*, 281–293.

Received: August 8, 2010
Revised: September 8, 2010
Published online:

